HHS Public Access

Author manuscript

J Nat Prod. Author manuscript; available in PMC 2021 August 09.

Published in final edited form as:

J Nat Prod. 2020 May 22; 83(5): 1553–1562. doi:10.1021/acs.jnatprod.0c00025.

Spongian Diterpenoids Derived from the Antarctic Sponge *Dendrilla antarctica* Are Potent Inhibitors of the *Leishmania* Parasite

Andrew J. Shilling,
Department of Chemistry, University of South Florida, Tampa, Florida 33620, United States

Christopher G. Witowski,
Department of Chemistry, University of South Florida, Tampa, Florida 33620, United States

J. Alan Maschek,
Department of Chemistry, University of South Florida, Tampa, Florida 33620, United States

Ala Azhari,
Department of Global Health, University of South Florida, Tampa, Florida 33612, United States;

Department of Microbiology and Medical Parasitology, King Abdulaziz University, Jeddah 22252, Saudi Arabia

Brian A. Vesely,
Department of Global Health, University of South Florida, Tampa, Florida 33612, United States

Dennis E. Kyle,
Department of Global Health, University of South Florida, Tampa, Florida 33612, United States

Charles D. Amsler,
Department of Biology, University of Alabama at Birmingham, Birmingham, Alabama 35294, United States

James B. McClintock,
Department of Biology, University of Alabama at Birmingham, Birmingham, Alabama 35294, United States

Bill J. Baker
Department of Chemistry, University of South Florida, Tampa, Florida 33620, United States

Abstract

Corresponding Author: Bill J. Baker – Department of Chemistry, University of South Florida, Tampa, Florida 33620, United States; Phone: +1 (813) 974-1967; bjbaker@usf.edu; Fax: +1 (813) 974-2876.

Supporting Information

The Supporting Information is available free of charge at https://pubs.acs.org/doi/10.1021/acs.jnatprod.0c00025.

^{1}H, ^{13}C, 2D NMR, and HRESIMS spectra for membranoids B–H (**6**–**12**) (PDF)

X-ray crystallographic metadata for membranoid C (**7**) (CIF)

X-ray crystallographic metadata for membranoid D (**9**) (CIF)

X-ray crystallographic metadata for membranoid G (**11**) (CIF)

Complete contact information is available at: https://pubs.acs.org/10.1021/acs.jnatprod.0c00025

The authors declare no competing financial interest.

From the CH_2Cl_2 extract of the Antarctic sponge *Dendrilla antarctica* we found spongian diterpenes, including previously reported aplysulphurin (**1**), tetrahydroaplysulphurin-1 (**2**), membranolide (**3**), and darwinolide (**4**), utilizing a CH_2Cl_2/MeOH extraction scheme. However, the extracts also yielded diterpenes bearing one or more methyl acetal functionalities (**5**–**9**), two of which are previously unreported, while others are revised here. Further investigation of diterpene reactivity led to additional new metabolites (**10**–**12**), which identified them as well as the methyl acetals as artifacts from methanolysis of aplysulphurin. The bioactivity of the methanolysis products, membranoids A–H (**5**–**12**), as well as natural products **1**–**4**, were assessed for activity against *Leishmania donovani*-infected J774A.1 macrophages, revealing insights into their structure/activity relationships. Four diterpenes, tetrahydroaplysulphurin-1 (**2**) as well as membranoids B (**6**), D (**8**), and G (**11**), displayed low micromolar activity against *L. donovani* with no discernible cytotoxicity against uninfected J774A.1 cells. Leishmaniasis is a neglected tropical disease that affects one million people every year and can be fatal if left untreated.

Graphical Abstract

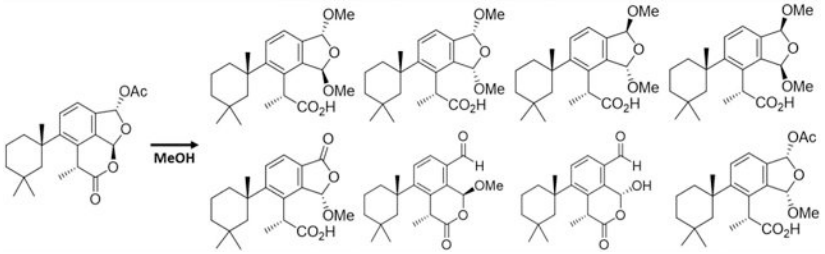

The sponge *Dendrilla membranosa* has been the subject of a number of chemical investigations resulting in reports of over a dozen rearranged and oxidized spongian diterpenes.[1–6] Though there are numerous reports of chemistry isolated from individuals collected in Antarctica, it has recently been suggested that these belong to a distinct species endemic to the southernmost continent, which we will herein refer as *Dendrilla antarctica*.[7] Some evidence of location-dependent chemodiversity variation is found in these reports with diterpene profiles seemingly representative of collection site around the continent. We have previously reported that specimens found near Palmer Station, Antarctica, produce primarily spongian diterpenes aplysulphurin (**1**), tetrahydroaplysulphurin-1 (**2**), and membranolide (**3**).[2] More recently we reported darwinolide (**4**),[5] a rearranged spongian diterpene from the same *D. antarctica* population near Palmer Station, demonstrating that chemodiversity plasticity is in fact phenotypic. Our 2001 collection noted[2] three minor bis(methyl acetal) derivatives (**5**, **7**, **9**) of aplysulphurin which have demonstrated variable concentrations in subsequent studies of the sponge.

Spongian diterpenes display a variety of pharmacological properties, including cytotoxicity and antibiotic and anti-inflammatory activity,[8] though they are rarely potent or selective. In a screening campaign for natural products active against the leishmaniasis parasite, *Leishmania donovani*, we found four diterpenoids from a *D. antarctica* extract, tetrahydroaplysulphurin-1 (**2**) as well as membranoids B (**6**), D (**8**), and G (**11**), that are both very potent and highly selective for parasite-infected cells over host mammalian cells.

L. donovani is a neglected tropical disease spread by sandflies affecting millions of people per year and can be fatal in its visceral form if left untreated.[9] Intravenous amphotericin is the only currently approved treatment for visceral leishmaniasis in the US,[9] though interest in new treatments is strong.[10–13] The bis(methyl acetal) membranoid scaffold seen in membranoids B–E (**6**–**9**) represents an intriguing model in functionality that could serve as the basis of future studies to enhance their therapeutic potential.

D. antarctica collected near Palmer Station, Antarctica, was reported in 2004 to produce diterpene metabolites including aplysulphurin (**1**), tetrahydroaplysulphurin-1 (**2**), membranolide (**3**), and the three methyl acetal membranolide derivatives (**5**, **7**, **9**) termed membranolides B–D.[2] When our *L. donovani* screening program identified *D. antarctica* extract as active, we began the analysis of additional specimens of this sponge and report here revisions of stereochemical assignments and NMR shifts of the two originally published bis(methyl acetal) compounds (**7** and **9**) as well as further methyl acetal and hemiacetal derivatives of membranolide (**6**, **8**, **10**–**12**).

Besides previously characterized bis(methyl acetal) derivatives **7** and **9**, the new sponge specimens yielded two additional bis(methyl acetal) derivatives, **6** and **8**, representing all four possible diastereomeric bis(methyl acetal) derivatives. Such a display of methyl acetals led us to reinvestigate the reactivity of *D. antarctica* spongian diterpenes toward alcoholic solvents. We found aplysulphurin alone among *D. antarctica* diterpenes is sensitive to MeOH, but not other alcohols.[2] That diterpenes **5**–**12** can be obtained by treatment of aplysulphurin with MeOH leads us to conclude these *D. antarctica* methyl acetals (and one hemiacetal) are artifacts, derived from using methanolic solvent mixtures in the extraction protocol. In the current study, spongian diterpenes **1**–**5** were characterized based on comparison of their spectroscopic data with published data.[2,3,14,15] X-ray crystal structures obtained of the previously isolated bis(methyl acetal) derivatives **7** and **9** forced us to re-examine and revise their configurational assignments and spectroscopic data. We introduce the name membranoids for all MeOH adducts, which requires renaming membranolides B–D[2] (**5**, **7**, **9**) as membranoids A, C, and E, while new derivatives **6**, **8**, and **10**–**12** are referred to as membranoids B, D, F, G, and H, respectively. Characterization of compounds **6**–**12** is reported here along with biological evaluation of natural and artifactual diterpenes for the control of the leishmaniasis parasite, *L. donovani*.

RESULTS AND DISCUSSION

Chemical Analysis.

This study began with a 1:1 CH_2Cl_2/MeOH extract derived from 330 g of freeze-dried *D. antarctica* collected in 2010. The 20% EtOAc/hexanes fraction from MPLC analysis was subjected to reversed-phase HPLC (60% acetonitrile in water), providing previously unreported bis(methyl acetal) membranoids B (**6**) (5.3 mg) and D (**8**) (22.2 mg). For comparison, the same MPLC fraction, upon further HPLC, also yielded membranolide (**3**, 19.3 mg), membranoids C and E (**7**, 4.8 mg; **9**, 19.9 mg), and tetrahydroaplysulphurin-1 (**2**, 52.3 mg).

Membranoid B (**6**) was obtained as a clear oil with spectroscopic data very similar to that of the previously reported bis(methyl acetal) metabolites.[2] A formula of $C_{22}H_{32}O_5$ was established from HRESIMS. Key ^{1}H NMR signals (Table 1) include a *gem*-dimethyl group, H_3-18 (δ_H 0.36) and H_3-19 (δ_H 0.90), and a singlet methyl at H_3-20 (δ_H 1.44), all of which are shown to be substituents on a trimethylcyclohexyl ring via HMBC correlations of H_3-18, H_3-19, and H_3-20 to alkyl carbon C-5 (δ_C 51.0) and correlations of H_3-18 and H_3-19 to C-3 (δ_C 39.6), which is connected to C-1 (δ_C 41.2) through a COSY spin system involving H_2-3 (δ_H 1.27), H-2α (δ_H 1.64), H-2β (δ_H 1.78), H-1α (δ_H 1.45), and H-1β (δ_H 2.32). Further HMBC correlations of H_3-20 to C-1 and C-9 (δ_C 148.5) established the trimethylcyclohexyl ring as a substituent on a phenyl ring that also bears two COSY linked adjacent aromatic protons, H-11 (δ_H 7.58) and H-12 (δ_H 7.24). HMBC correlations of a doublet methyl at H_3-17 (δ_H 1.58; J = 7.2) and its coupled quartet methine at H-7 (δ_H 4.64, J = 7.0) to both the carboxylic acid C-6 (δ_C 178.8) and aromatic carbon C-8 (δ_C 135.7) verifies a propanoic acid substituent on the phenyl ring, and additional HMBC correlations of H-7 to C-9 and H-11 to C-8 establish it adjacent on the phenyl ring to the trimethylcyclohexyl group. Two acetal methine signals, H-15 (δ_H 6.32) and H-16 (δ_H 6.24), along with two overlapping methoxy groups, H_3-21 (δ_H 3.40) and H_3-22 (δ_H 3.40), are characteristic of the bis(methyl acetal)-fused furano-membranoids. The coincident methoxy signals are resolved in CD_3CN at H_3-21 (δ_H 3.26) and H_3-22 (δ_H 3.30), respectively (Figure S7). HMBC correlations of H_3-21 to C-15 (δ_C 106.2) and H_3-22 to C-16 (δ_C 105.9), as well as H-15 to C-16, establish the methyl acetal positions about the dihydrofuran ring and are supported in their locations as substituents on the phenyl ring by HMBC correlations of H-15 to C-13 (δ_C 137.1) and H-16 to C-12 (δ_C 121.4) and C-14 (δ_C 138.4).

The three additional bis(methyl acetal) membranoids (**7**–**9**) shared ^{1}H and ^{13}C shifts (Table 1) and connectivity (Figure 1) with membranoid B (**6**). Membranoid C (**7**) was obtained as a clear oil with spectroscopic data (Table 1) consistent with that previously published as membranolide C.[2] A formula of $C_{22}H_{32}O_5$ was established based on HRESIMS. The ^{1}H and ^{13}C NMR data and 2D NMR connectivity and correlations unambiguously established the planar structure for membranoid C as that of the bis(methyl acetal) fused furano-membranoids as depicted for membranoid B in Figure 1 and supports the previously reported two-dimensional structure.[2] Membranoid D (**8**) was likewise obtained as a clear oil with a formula of $C_{22}H_{32}O_5$ established based on HRESIMS. The ^{1}H and ^{13}C NMR data and 2D NMR connectivity and correlations also established the planar structure for membranoid D as that of the bis(methyl acetal)-fused furano-membranoids (Figure 1). The last of the four possible diastereomers, membranoid E (**9**), was similarly obtained as a clear oil with NMR data (Table 1) nearly identically matched with that of previously published membranolide D, with the exception of the acetal methine ^{1}H NMR shifts of H-15 and H-16, which were originally reported as overlapping singlets at 6.20 ppm in $CDCl_3$.[2] We have reviewed the data and note the same overlapping acetal methine signals in membranoid E (**9**) occurring at 6.02 ppm and have determined the original report incorrectly reported the 6.02 ppm shift as 6.20 ppm. As with **6**–**8**, a formula of $C_{22}H_{32}O_5$ was established for **9** based on HRESIMS, and the ^{1}H and ^{13}C NMR data and 2D NMR connectivity and correlations definitively support the previously reported two-dimensional structure (Figure 1).[2]

The relative and absolute configurations of the four bis(methyl acetal) fused furanomembranoids were ascertained using a combination of X-ray crystallography and 1D and 2D NMR data and have resulted in the reassignment of some of the originally reported structures.[2] Slow evaporation from 4:1 hexane/EtOAc at −80 °C over 9 months afforded crystals of membranoid C (**7**) suitable for X-ray crystallographic analysis. The crystallographic metadata (Flack parameter −0.03(7)), Bijvoet-pair analysis, and Bayesian statistics method (P2 (true) = 1; P3 (true) = 1; P3 (false) = 0.2×10^{-58}; P3 (rac-twin) = 0.1×10^{-14} (Table S4)) supported the assignment of the configuration depicted in Figure 2 as the absolute configuration of membranoid C (**7**). This configuration revises the original published structure for membranolide C from an (*R,R*) configuration about stereocenters C-15 and C-16, respectively,[2] to (*S,R*), establishing a new *α-cis* orientation of the methoxy substituents and *β-cis* orientation of the acetal methines about the dihydrofuran ring for membranoid C (**7**).

Similarly, slow evaporation from 4:1 hexane/EtOAc at −80 °C, this time over 12 months, afforded crystals of membranoid E (**9**) for X-ray analysis. The crystallographic metadata (Flack parameter −0.01(8)), Bijvoet-pair analysis, and Bayesian statistics method (P2 (true) = 1; P3 (true) = 1; P3 (false) = 0.7×10^{-37}; P3 (rac-twin) = 0.4×10^{-9} (Table S4)) established the configuration depicted in Figure 3 as the absolute configuration of membranoid E (**9**). The asymmetric unit found by X-ray spectroscopy includes two molecules of **9** disposed as H-bonded mirror-images about the carboxylic acid groups. The data support the originally reported (*R,S*) configuration about stereocenters C-15 and C-16, respectively, and *β-cis* orientation of the methoxy substituents about the dihydrofuran ring.[2]

Because both of the *cis*-bis(methyl acetal) diastereomers are accounted for by membranoids C (**7**) and E (**9**), both membranoid B (**6**) and membranoid D (**8**) must display a *trans*-orientation about the dihydrofuran ring. Examination of the overlapping ^{1}H NMR shifts of the H-15 and H-16 acetal methines of the *cis* diastereomers reveals a trend in which the *β*-orientation of the acetal methines as seen in **7** results in a more shielded shift for both positions (δ_H 5.89) relative to the *α*-orientation seen in **9**, which are more deshielded (δ_H 6.02). The acetal methine ^{1}H NMR shifts seen in membranoid B (**6**) and membranoid D (**8**) reflect this trend and support a *trans* configuration about the dihydrofuran ring for both compounds (Table 1). In membranoid B (**6**), H-15 (δ_H 6.32) appears more deshielded relative to H-16 (δ_H 6.24), indicating an (*R,R*) conformation about stereocenters C-15 and C-16, respectively, with an *α*-orientation for H-15 and *β*-orientation for H-16. Observation of a NOESY correlation obtained in CD_3CN between H-15 (δ_H 6.26) and H_3-17 (δ_H 1.52) supports the *α*-orientation for H-15 (Figure 4). Conversely membranoid D (**8**) displays H-15 (δ_H 6.12) appearing more shielded relative to H-16 (δ_H 6.31), representing an (*S,S*) conformation about stereocenters C-15 and C-16, respectively, with an *β*-orientation for H-15 and *α*-orientation for H-16. Observation of a ROESY correlation between H_3-21 (δ_H 3.45) and H_3-17 (δ_H 1.71) supports the *α*-orientation for H_3-21 (Figure 4).

Treatment of Spongian Diterpenes with MeOH.

Isolation of the four bis(methyl acetal) diastereomers led us once again[2] to consider the artifactual nature of the compounds. Extraction of *D. antarctica* in the absence

of MeOH, using just CH_2Cl_2, produced an extract containing only aplysulphurin (**1**), tetrahydroaplysufphurin-1 (**2**), membranolide (**3**), and darwinolide (**4**). That extract, when stirred with MeOH for 12 h, displayed new products with masses and retention times consistent with the membranoids. Similarly, purified aplysulphurin, the only natural product present in the extract with the same oxidation state as the membranoids, was similarly treated with MeOH and demonstrated (Figure 5) to convert to a mixture of new compounds bearing appropriate masses (*m*/*z* 345.2064 $[M + H]^+$; *m*/*z* 399.2148 $[M + Na]^+$; 361.1982 $[M + H]^+$) of membranoids **5**–**10**.

Purification of the reaction products from methanolysis of aplysulphurin resulted in the isolation of membranoids A (**5**, 20.8%), B (**6**, 4.2%), C (**7**, 1.3%), D (**8**, 3.8%), and E (**9**, 2.9%), along with new compounds membranoids F (**10**, 2.1%) and G (**11**, 0.8%). Unreacted aplysulphurin (60%) was also recovered. Membranoid F (**10**) was isolated as a clear oil with a molecular formula established as $C_{21}H_{28}O_5$ through HRESIMS. The 1H NMR spectrum (Table 2) exhibited several key signals characteristic of the membranoid series including two doublet aromatic protons at δ_H 7.73 and δ_H 7.76 (H-11; H-12; J = 8.3 Hz) consistent with a tetrasubstituted phenyl ring, as well as doublet methyl H_3-17 (δ_C 1.73; J = 7.3 Hz), *gem*-dimethyl H_3-18 (δ_H 0.48) and H_3-19 (δ_H 0.95), and singlet methyl H_3-20 (δ_H 1.42) groups. The anomalous shielded chemical shift for H_3-18 again identified it as the axial methyl signal on C-4 of the cyclohexane ring, which is characteristic of the 1′,3′,3′-trimethylcyclohexylbenzene system due to the proximity of the axial methyl in the anisotropic shielding zone of the aromatic ring.[15] Assignment of the membranoid F planar structure was completed via HMBC correlations and comparison of ^{13}C NMR data to that of previously reported compounds.[2,3,15] For example, connectivity to the aromatic ring from C-10 (δ_C 40.3) was established via HMBC correlations from H_3-20 to aromatic C-9 (δ_C 154.9) (Figure 6). Methine singlet H-15 (δ_H 6.14) displays HMBC correlations to a lactone-type C-16 (δ_C 168.6) as well as C-21 (δ_C 56.5) and C-13 (δ_C 126.0), establishing the connectivity of the methoxy furanone moiety to the aromatic ring. Consistent with previous studies, spatial arrangement of methyl doublet H_3-17 and methine quartet H-7 (δ_H 4.73; J = 6.7) was established via ROESY correlations of H-7 to H-5β (δ_H 2.13) (e.g., Figure 6).[14] The configuration of the methoxy furanone was established by observation of a ROESY correlation between H_3-17 and H_3-21 (δ_H 3.59), establishing an α-orientation of the C-15 methyl acetal.

Membranoid G (**11**) was isolated as a clear oil with a molecular formula of $C_{20}H_{26}O_4$ established by HRESIMS. The ^1H and ^{13}C NMR data (Table 2) exhibited general features similar to those observed for **5** including an aldehyde singlet H-16 (δ_H 10.1), doublet methyl H_3-17 (δ_H 1.87; J = 7.1 Hz), *gem*-dimethyl H_3-18 (δ_H 0.58) and H_3-19 (δ_H 0.97), and a singlet methyl H_3-20 (δ_H 1.32). It was, however, lacking the H_3-21 methoxy group and instead bears a hydroxy group (δ_H 5.00). The only other significant difference observed in the ^1H NMR data was at position C-15, where the methine shift at δ_H 7.26 (H-15) differs by 0.46 ppm compared to **5**, suggesting **11** is similar but contains a hemiacetal at C-15 instead of a methyl acetal. This is supported by HMBC correlations of H-15 to C-6 (δ_C 174.3), C-8 (δ_C 138.2), and C-13 (δ_C 130.5), establishing the hemiacetal at the C-15 position within the lactone ring. Additional correlations of H-12 to C-16 (δ_C 192.5) and H-16 to C-13 (δ_C

130.5) and C-14 (δ_C 134.0) place the aldehyde as a substituent on the benzene ring at the C-16 position. In 1984 Karuso et al. in fact reported[14] the hemiacetal equivalent structure to **5** as a semisynthetic derivative obtained by heating aplysulphurin in wet DMSO and purified using HPLC; however, the aldehyde reported in that paper differs from **11** in its doublet methyl shift (H_3-17) by 0.19 ppm, suggesting that membranoid G (**11**) could be a diastereomer, a notion that is supported by observation of a NOESY correlation between H_3-17 and the proton of the hydroxy group (Figure 7).

Acquisition of an X-ray crystal structure confirmed membranoid G (**11**) to be epimeric at the C-15 center to the compound originally described by Karuso et al., 1984, with the difference in the doublet methyl shift (H_3-17) likely due to the deshielding effect of its closer three-dimensional proximity to the hemiacetal hydroxy group (Figure 8). Large pristine crystals ideal for X-ray crystallographic analysis were grown by slow cooling of a saturated solution in a 9:1 mixture of hexane/CH_2Cl_2 from 25 °C down to a temperature of 10 °C over a period of 10 days. The crystallographic metadata (Flack parameter −0.13(15)), Bijvoet-pair analysis, and Bayesian statistics method (P2 (true) = 1; P3 (true) = 1; P3 (false) = 0.3 × 10^{-17}; P3 (rac-twin) = 0.4 × 10^{-5} (Table S4)) established the configuration depicted in Figure 8 as the absolute configuration of membranoid G, displaying an (*R*) conformation about stereocenter C-15, with the hemiacetal methine in the β-orientation.

A subsequent methanolysis reaction, increased by an order of magnitude to a 250 mg scale, produced similar yields of membranolides A–G, except that no membranoid F was recovered and a new membranoid, membranoid H (**12**, 7.1%), was found. We have noted in subsequent observations of the methanolysis reaction that membranoid H is not isolated from the mixture if the reaction is allowed to stir for long periods (>48 h). Furthermore, membranoid H degraded to a binary mixture of membranoids A (**5**) and G (**11**) upon standing in chloroform for 72 h, leading us to believe membranoid H is a reactive intermediate that is formed early in the reaction and eventually progresses to the other products. Similarly, if left in chloroform over several months, the bis(methyl acetal) membranoids (**6**–**9**) will also degrade to a mixture of the two aldehydes **5** and **11**.

Membranoid H (**12**) was obtained as a clear oil with spectroscopic data similar to those of membranoids B–E (**6**–**9**) but containing an additional carbon and oxygen. A formula of $C_{23}H_{32}O_6$ was established from HRESIMS. Key ^{1}H NMR signals (Table 2) include a *gem*-dimethyl group at H_3-18 (δ_H 0.47) and H_3-19 (δ_H 0.93), a singlet methyl at H_3-20 (δ_H 1.38), a doublet methyl at H_3-17 (δ_H 1.63; J = 7.1), a quartet methine at H-7 (δ_H 4.64, J = 7.2), and the pair of aromatic protons at H-11 (δ_H 7.65) and H-12 (δ_H 7.30) and establish this structure as the membranoid scaffold. Two acetal methine signals at H-15 (δ_H 5.86) and H-16 (δ_H 6.98) indicate this as a fused furano-membranoid supported in their positions by HMBC correlations of H-15 to C-13 (δ_C 137.5) and H-16 to C-12 (δ_C 130.2) and C-14 (δ_C 140.8). Signals establishing the substituents about the dihydrofuran ring include one methoxy group at H_3-21 (δ_H 3.39) and one acetate methyl at H_3-23 (δ_H 2.06), supported in their positions by HMBC correlations of H-15 to C-21 (δ_C 55.3), and H-16 to C-22 (δ_C 171.2) as well as H_3-23 to C-22. The relative configuration of the fused dihydrofuran ring of **12** was established by observation of a NOESY correlation between H_3-17 and H_3-21 (δ_H 3.39), establishing the same α-relationship of the C-15 methyl acetal as was observed

in membranoid F (**10**). An additional NOESY correlation was observed between H_3-21 and H_3-23, indicating a *cis* conformation and α-orientation of the methoxy and acetate groups about the dihydrofuran ring (Figure 9).

The reactivity of aplysulphurin (**1**) is enigmatic, likely driven by the densely functionalized central aromatic ring in a constrained trifused 6/6/5 system. The X-ray structure[16] depicts a congested central aromatic ring in the axial position of a trimethylcyclohexane ring, a concave orientation that largely blocks the α-face and produces anisotropic NMR shifts described previously.[14] That MeOH, but not EtOH,[2] induces solvolysis emphasizes the congestion. Further studies of the mechanistic aspects of solvolysis that explain the cascade of products are currently ongoing.

Leishmaniasis Activity of *D. antarctica*-Derived Compounds.

The full suite of *D. antarctica*-derived compounds were tested against *L. donovani*-infected macrophages. Companion cytotoxicity measurements were conducted using the host mammalian J774A.1 cell line. The results (Table 3) suggest modest activity (lower activity than the miltefosine positive control) for membranolide (**3**, 9.7 μM), darwinolide (**4**, 11.2 μM), and membranoids C (**7**, 6.5 μM), E (**9**, 6.6 μM), and H (**12**, 12.0 μM), but potent bioactivity (greater activity than the miltefosine positive control) for aplysulphurin (**1**, 3.10 μM) and tetrahydroaplysulphurin-1 (**2**,3.50 μM), as well as membranoids B (**6**, 0.8 μM), D (**8**, 1.40 μM), and G (**11**, 2 μM). In addition, a high selectivity index (SI, mammalian cytotoxicity/antiprotozoal activity) was observed for **2** (>38), **6** (>166), **8** (>95), and **11** (>100). Three of these potent and selective hits (**6**, **8**, **11**) are newly reported artifacts, showing greater antileishmanial activity than the standard treatment of miltefosine (2.9 μM), and are more active and far more selective than the aplysulphurin precursor (**1**, 3.10 μM, SI 4.0). To our surprise, both of the *cis* methyl acetals membranoids C (**7**) and E (**9**) were less active against *L. donovani*-infected macrophages compared with their diastereomers **6** and **8**, which are both *trans* about the dihydrofuran ring. This makes the functionality and orientation of these substituents at positions C-15 and C-16 crucial for *L. donovani* bioactivity and could represent a feasible starting point for further SAR studies utilizing the membranoid backbone. Another interesting trend is observed in the stark contrast between the activity and selectivity of membranoids A (**5**) and G (**11**). While they are structurally very similar, each bearing an aldehyde at the C-16 position and differing only in the relative configuration and functionality of the oxidized C-15 carbon, membranoid A (**5**) was inactive against *L. donovani*-infected macrophages at the highest concentrations tested and mildly toxic to the J774A.1 cells, while membranoid G showed potent activity against the infection with no discernible cytotoxicity against healthy mammalian cells. This could also represent a promising motif practicable for optimization through SAR.

EXPERIMENTAL SECTION

General Experimental Procedures.

Optical rotations were measured on a Rudolph Research Analytical AUTOPOL IV digital polarimeter. UV absorptions were measured by an Agilent Cary 60 UV–vis spectrophotometer in MeOH or MeCN, while IR spectra were recorded with an Agilent

Cary 630 FTIR. All NMR spectra were acquired in $CDCl_3$ or CD_3CN with residual solvent referenced as an internal standard (7.27 and 1.94 ppm for ^1H and 77.0 and 1.29 ppm for ^{13}C, respectively). All ^1H NMR spectra were recorded on a Varian 500 or 600 MHz Direct Drive instrument equipped with cold-probe detection, and ^{13}C NMR spectra were recorded at 125 or 150 MHz, respectively. Analytical LC/MS was performed on a Phenomenex Kinetex C18 column (50 × 2.1 mm, 2.6 μm) on either an Agilent 6120 single quadrupole, an Agilent 6230 LC/ToF-MS, or an Agilent 6540 LC/QToF-MS with electrospray ionization detection, the latter two of which were utilized for HRESIMS. All HPLC analysis was performed on a Shimadzu LC20-AT system equipped with a photodiode array detector (M20A) using semipreparative [Phenomenex Luna C18 (250 × 10 mm, 5 μm)] or analytical [Phenomenex Luna C18 (250 × 4.6 mm, 5 μm) and Phenomenex Luna Silica (250 × 4.6 mm, 5 μm)] conditions. All solvents were obtained from Fisher Scientific and were HPLC grade (>99% purity) unless otherwise stated.

Collection of *D. antarctica*.

Sponge samples were collected from various sites around Palmer Station, Antarctica, in the Austral summers of 2010, 2011, and 2016. The collection sites chosen were Norsel Point (64°45.674′ S, 64°05.467′ W), Bonaparte Point (64°46.748′ S, 64°02.542′ W), Gamage Point (64°46.345′ S 64°02.915′ W), and Laggard Island (64°48.568′ S, 64°00.984′ W) at depths between 5 and 35 m. Samples were frozen and transported back to the University of South Florida at −70 °C, where tissues were lyophilized and stored at −80 °C until further processing. Specimens examined by Professor Rob van Soest, then at the University of Amsterdam, were previously[2,6] identified as *Dendrilla membranosa*. More recent consideration[7] suggests specimens of this sponge originating in Antarctica should be identified as *D. antarctica*. Previous reports of chemistry from Antarctic *D. membranosa* should be considered as originating from the same sponge species as studied here.

Extraction and Isolation of Natural Products.

A typical CH_2Cl_2/MeOH (1:1) extraction was conducted on the 2010 collection. From 330 g of freeze-dried *D. antarctica*, 12.2 g of CH_2Cl_2/MeOH was obtained and subsequently fractionated by NP MPLC into 11 fractions using a linear gradient from hexanes to EtOAc to MeOH. The third through fifth fractions, eluting roughly between 20% and 50% EtOAc in hexanes, contained diterpenes. The diterpene fractions were combined, and a 400 mg aliquot separated on RP HPLC using 60% MeCN in water to 100% MeCN. In order of elution were obtained membranoid E (**9**, 4.8 mg), B (**6**, 19.9 mg), D (**8**, 5.3 mg), and C (**7**, 22.2 mg), as well as natural products membranolide (**3**, 19.3 mg) and tetrahydroaplysulphurin-1 (**2**, 52.3 mg).

Similarly, a typical CH_2Cl_2 extraction is illustrated by a 25.7 g sample of freeze-dried *D. antarctica*, which was extracted three times with CH_2Cl_2 (ACS grade), and the combined extracts were concentrated *in vacuo*. The lipophilic extract (994 mg) was absorbed onto Waters Sep-Pak C18 cartridges and eluted with MeCN. The dried eluate (205 mg) was separated by isocratic semipreparative HPLC using 60% MeCN in H_2O for 35 min and ramping up to 100% MeCN after 50 min to afford (in retention time order) membranolide

(**3**, 8.7 mg), aplysulphurin (**1**, 10.2 mg), tetrahydroaplysulphurin-1 (**2**, 1.5 mg), and darwinolide (**4**, 2.0 mg).

Methanolysis of Aplysulphurin.

Aplysulphurin (**1**) was dissolved to 1 mg/mL in MeOH; 10 μL aliquots were taken at time zero and then every 3 h. Those aliquots were transferred to LCMS vials, dried under nitrogen, and resuspended in 1 mL of acetonitrile. Sample analysis was performed via LC/QToF-MS with a gradient of 40–60% acetonitrile in water (0.1% formic acid) over 7 min, before a ramp to 100% acetonitrile for 10 min.

Isolation of Membranoids.

Previously purified aplysulphurin (**1**, 24.0 mg) treated with MeOH for 48 h was subject to semipreparative RP HPLC using a 60–65% MeCN in H_2O gradient over 30 min followed by NP analytical HPLC with 10–100% EtOAc in hexane, yielding membranoid A (**5**, 5.0 mg), membranoid B (**6**, 0.7 mg), membranoid C (**7**, 0.3 mg), membranoid D (**8**, 0.9 mg), membranoid E (**9**, 1.0 mg), membranoid F (**10**, 0.5 mg), and membranoid G (**11**, 0.2 mg). No membranoid H (**12**) was isolated.

The methanolysis was then scaled up by an order of magnitude, stirring 250 mg of aplysulphurin (**1**) in MeOH at 1 mg/mL for 24 h. The MeOH was then removed under reduced pressure, and the mixture was subjected to semipreparative NP HPLC, this time using a 10–50% EtOAc in hexane gradient over 30 min, which was sufficient to achieve separation of the products. This yielded membranoid A (**5**, 27.3 mg), membranoid B (**6**, 8.8 mg), membranoid C (**7**, 19.9 mg), membranoid D (**8**, 23.5 mg), membranoid E (**9**, 10.5 mg), membranoid G (**11**, 0.7 mg), and membranoid H (**12**, 17.7 mg). The membranoid H (**12**) isolated from the scale up degraded to a binary mixture of membranoids A (**5**, 7.3 mg) and G (**11**, 7.1 mg) upon solvation in $CHCl_3$ over a 72 h period, and each was purified under the same NP HPLC conditions and confirmed by NMR data.

Membranoid B (6): clear oil; $[\alpha]^{20}_D$ −87 (c 0.6, $CHCl_3$); UV (MeOH) λ_{max} (log ε) 269 nm (3.57); IR ν (thin film) 2940, 1733, 1698, 1585, 1467, 1382 cm^{-1}; ^1H and ^{13}C NMR data, Table 1; HRESIMS m/z 399.2139 $[M + Na]^+$ (calcd for 399.2142, $C_{22}H_{32}O_5Na$).

Membranoid C (7): clear oil that crystallized on long-standing; $[\alpha]^{20}_D$ −100 (c 0.6, $CHCl_3$); UV (MeOH) λ_{max} (log ε) 267 nm (3.31); IR ν (thin film) 2940, 1733, 1698, 1585, 1467, 1382 cm^{-1}; ^1H and ^{13}C NMR data, Table 1; HRESIMS m/z 399.2141 $[M + Na]^+$ (calcd for 399.2142, $C_{22}H_{32}O_5Na$).

Membranoid D (8): clear oil; $[\alpha]^{20}_D$ +33 (c 0.6, $CHCl_3$); UV (MeOH) λ_{max} (log ε) 267 nm (3.41); IR ν (thin film) 2940, 1733, 1698, 1585, 1467, 1390 cm^{-1}; ^1H and ^{13}C NMR data, Table 1; HRESIMS m/z 399.2145 $[M + Na]^+$ (calcd for 399.2142, $C_{22}H_{32}O_5Na$).

Membranoid E (9): clear oil that crystallized on long-standing; $[\alpha]^{20}_D$ −37 (c 0.6, $CHCl_3$); UV (MeOH) λ_{max} (log ε) 269 nm (3.48); IR ν (thin film) 2940, 1733, 1698,

1585, 1467, 1382 cm^{-1}; ^{1}H and ^{13}C NMR data, Table 1; HRESIMS m/z 399.2140 $[M + Na]^+$ (calcd for 399.2142, $C_{22}H_{32}O_5Na$).

Membranoid F (10): clear oil; $[\alpha]^{20}_D$ +135 (c 0.14, $CHCl_3$); UV (MeOH) λ_{max} (log ε) 223 nm (3.32); ^{1}H and ^{13}C NMR data, Table 2; HRESIMS m/z 383.1821 $[M + Na]^+$ (calcd for 383.1829, $C_{21}H_{28}O_5Na$).

Membranoid G (11): clear oil that could be crystallized on long-standing; $[\alpha]^{20}_D$ −50 (c 0.14, $CHCl_3$); UV (MeOH) λ_{max} (log ε) 259 nm (3.71); IR ν (thin film) 3340, 2940, 2865, 1740, 1698, 1585, 1462, 1390 cm^{-1}; ^{1}H and ^{13}C NMR data, Table 2; HRESIMS m/z 353.1723 $[M + Na]^+$ (calcd for 353.1723, $C_{20}H_{26}O_4Na$).

Membranoid H (12): clear oil; $[\alpha]^{25}_D$ +50 (c 0.17, MeCN); UV (MeCN) λ_{max} (log ε) 264 nm (3.38); IR ν (thin film) 2940, 1740, 1704, 1472, 1385 cm^{-1}; ^{1}H and ^{13}C NMR data, Table 2; HRESIMS m/z 427.2089 $[M + Na]^+$ (calcd for 427. 2091 $C_{23}H_{32}O_6Na$).

X-ray Crystallography.

Crystals of **7** and **9** were obtained from EtOAc/hexane, while crystals of **11** were grown in CH_2Cl_2/hexane. The X-ray diffraction data were measured on a Bruker D8 Venture PHOTON II CPAD diffractometer equipped with a Cu Kα INCOATEC ImuS microfocus source (λ = 1.541 78 Å). Indexing was performed using APEX3 (Difference Vectors method).[17] Data integration and reduction were performed using SaintPlus.[18] Absorption correction was performed by the multiscan method implemented in SADABS.[19] Space group was determined using XPREP implemented in APEX3.[17] Structure was solved using SHELXT and refined using SHELXL-2018 (full-matrix least-squares on F^2) through the OLEX2 interface program.[20–22] All molecules are conformationally strained: corresponding hydrogen atoms were refined with restraints and with U_{iso} = 1.2C_{eq} (1.5 for the $-CH_3$ group). All other hydrogen atoms were placed in geometrically calculated positions and were included in the refinement process using a riding model with isotropic thermal parameters. Absolute configuration for all compounds was established based on the Flack parameter value and verified additionally with Bijvoet-pair analysis and Bayesian statistics methods (Table S4).[23,24] P2 = 1 for all cases and is the probability that the current model is correct assuming two possibilities: one out of two enantiomers present. Crystal data and refinement conditions are shown in Tables S1–S3.

Crystallographic Data for Membranoid C (7): $C_{22}H_{32}O_5$, M = 376.47, crystal size 0.14 × 0.079 × 0.054 mm^3, orthorhombic, a = 7.8794(2) Å, b = 13.8188(3) Å, c = 18.3689(4) Å, $\alpha = \beta = \gamma = 90°$, V = 2000.08(8) $Å^3$, T = 100 K, space group $P2_12_12_1$, Z = 4, D_{calcd} = 1.250 g/cm^3, μ = 0.704 mm^{-1}, F(000) = 816.0, 4201 independent reflections (R_{int} = 0.0477, R_{sigma} = 0.0300). The final R_1 = 0.0305 ($I \geq 2\sigma(I)$), wR_2 = 0.0733 ($I \geq 2\sigma(I)$), R_1 = 0.0332 (all data), wR_2 = 0.0756 (all data), S = 1.064. The Flack parameter was −0.03(7).

Crystallographic Data for Membranoid E (9): $C_{22}H_{32}O_5$, M = 376.47, crystal size 0.097 × 0.09 × 0.037 mm^3, monoclinic, a = 13.4041(3) Å, b = 9.8471(2) Å, c = 16.3030(4)

Å, $\alpha = 90°$, $\beta = 105.2120(10)°$, $\gamma = 90°$, $V = 2076.46(8)$ Å^3, $T = 100$ K, space group $P2_1$, $Z = 4$, $D_{calcd} = 1.204$ g/cm^3, $\mu = 0.678$ mm^{-1}, $F(000) = 816.0$, 8629 independent reflections ($R_{int} = 0.0636$, $R_{sigma} = 0.0437$). The final $R_1 = 0.0363$ ($I \geq 2\sigma(I)$), $wR_2 = 0.0826$ ($I \geq 2\sigma(I)$), $R_1 = 0.0439$ (all data), $wR_2 = 0.0868$ (all data), $S = 1.046$. The Flack parameter was −0.01(8).

Crystallographic Data for Membranoid G (11): $C_{20}H_{26}O_4$, M = 330.41, crystal size 0.19 × 0.12 × 0.12 mm^3, orthorhombic, $a = 10.9817(4)$ Å, $b = 11.0246(4)$ Å, $c = 14.6564(5)$ Å, $\alpha = \beta = \gamma = 90°$, $V = 1773.23(11)$ Å^3, $T = 134.98$ K, space group $P2_12_12_1$, $Z = 4$, $D_{calcd} = 1.238$ g/cm^3, $\mu = 0.684$ mm^{-1}, $F(000) = 712.0$, 3513 independent reflections ($R_{int} = 0.0463$, $R_{sigma} = 0.0450$). The final $R_1 = 0.0385$ ($I \geq 2\sigma(I)$), $wR_2 = 0.0961$ ($I \geq 2\sigma(I)$), $R_1 = 0.0394$ (all data), $wR_2 = 0.0971$ (all data), $S = 1.056$. The Flack parameter was −0.13(15).

Crystallographic data for the structures reported in this paper have been deposited with the Cambridge Crystallographic Data Centre as supplementary publication nos. CCDC 1942687 for **7**, CCDC 1942688 for **9**, and CCDC 1942689 for **11**. Copies of the data can be obtained, free of charge, on application to the Director, CCDC, 12 Union Road, Cambridge CB2 1EZ, UK (tel: (+44) 1223-336-408; fax: (+44) 1223-336-033; or email: deposit@ccdc.cam.ac.uk).

Biological Assays.

Leishmania donovani Cell Line Infected Macrophage Assay.—

MHOM/SD/75/1246/130 *L. donovani* axenic amastigotes were cultured in RPMI 1640 at a pH of 5.5 with 7.5 g/L HEPES (Invitrogen Corp.), 5.86 g/L MES (Sigma-Aldrich), 2 g/L sodium bicarbonate (Fisher Scientific), 10 mg/L hemin (Sigma-Aldrich), 100 μM xanthine (Sigma-Aldrich), 40 mg/L Tween-80 (Sigma-Aldrich), 1% penicillin–streptomycin, 5 g/L Trypton-Peptone (BD Bioscience), and 20% 24 h heat-inactivated FBS. *L. donovani* was incubated at 37 °C. All culturing was done using nonvented 25 cm^2 tissue culture flasks (Corning). J774A.1 macrophages (ATCC) were cultured using RPMI 1640 (Gibco), 1% penicillin–streptomycin (Gibco, 10,000 u/mL), and 10% 24 h heat-inactivated fetal bovine serum (Gibco) at a pH of 7.2. All culturing was done using vented 75 cm^2 tissue culture flasks (Corning) and incubated at 37 °C, 5% CO_2.

In a 384-well plate (CellCarrier-384 black, optically clear bottom, tissue culture treated, sterile), 2000 J774A.1 cells were seeded. *L. donovani* axenic amastigotes (MHOM/SD/75/1246/130 cell line) were then added to the plate at a ratio of 10:1 and incubated at 37 °C, 5% CO_2 for 24 h. The excess extracellular amastigotes were then washed away using prewarmed media. Compounds **1**–**12**, in addition to the positive control miltefosine, were prepared in a 384-well plate (Thermo Scientific Nunc 384-well clear polystyrene plates (non/treated surfaces)) with a starting concentration of 10 μg/mL and serially diluted at 1:2. Drugs were then added to the assay plate and incubated at 37 °C, 5% CO_2 for 72 h. Cells were then fixed with 2% paraformaldehyde (Alfa Aesar paraformaldehyde, 16% w/v aqueous solution, MeOH free) and incubated for 15 min at room temperature, then stained with 5 μM Draq5 (Thermo Scientific DRAQ5 fluorescent probe) and incubated for 5 min at room temperature. A PerkinElmer Operetta (high-content imager) was used to capture images for each well and find macrophage and amastigote

nuclei within macrophage cytoplasm using Harmoney software that counts the number of amastigotes per 500 macrophages in each well and generated IC_{50} values.

Cytotoxicity Assay.—Cytotoxicity was determined by using a colorimetric assay where compounds **1**–**12** and the positive control miltefosine were tested against J774.A1 macrophages using the CellTiter 96 AQueous One solution cell proliferation assay (Promega). In a 96-well drug plate (Costar, assay plate, 96-well with low-evaporation lid, flat bottom, nontreated) drugs were diluted in a series of six 2-fold dilutions in media to produce a concentration range from 500 to 15.625 μg/mL. A 10 μL amount from each well was transferred to another 96-well plate (Costar, assay plate, 96-well with low-evaporation lid, flat bottom, tissue culture treated), and 90 μL of macrophages in media in a 50 000 cell per well concentration was added to produce a final concentration range from 50 to 1.6 μg/mL. The plates were then incubated at 37 °C, 5% CO_2 for 72 h. A 20 μL amount of 3-(4,5-dimethylthiazol-2-yl)-5(3-carboxymethoxyphenyl)-2-(4-sulphophenyl)-2*H*-tetrazolium (MTS: Promega) solution was added to each well and incubated for an additional 4 h. A Spectra Max M2e (Molecular Devices) was used to measure optical density at 490 nm. Nonlinear regression via Trifox software was used to determine IC_{50} values.

Supplementary Material

Refer to Web version on PubMed Central for supplementary material.

ACKNOWLEDGMENTS

This work was funded by the National Science Foundation awards ANT-0838773 and PLR-1341333 (C.D.A., J.B.M.) and ANT-0838776 and PLR-1341339 (B.J.B.) from the Antarctic Organisms and Ecosystems program and a Center of Excellence award from the State of Florida to support the Center for Drug Discovery and Innovation, whose facilities made much of the chemical analysis possible. We greatly appreciate the outstanding logistical support of the employees and subcontractors of Raytheon Polar Services Company and Antarctic Support Contract. We are appreciative of Dr. E. Rivera for assistance in obtaining high-quality NMR spectra and Dr. L. Wojtas, G. Verma, and C. Shan for assistance with X-ray crystallography. J.B.M. acknowledges the support of an Endowed Professorship from the University of Alabama at Birmingham.

REFERENCES

(1). Fontana A; Scognamiglio G; Cimino G J. Nat. Prod 1997, 60, 475–477.

(2). Ankisetty S; Amsler CD; McClintock JB; Baker BJ J. Nat. Prod 2004, 67, 1172–1174. [PubMed: 15270575]

(3). Molinski TF; Faulkner DJ J. Org. Chem 1987, 52, 296–298.

(4). Manriquez V; San-Martin A; Rovirosa J; Darias J; Peters K Acta Crystallogr., Sect. C: Cryst. Struct. Commun 1990, C46, 2486–2487.

(5). von Salm JL; Witowski CG; Fleeman RM; McClintock JB; Amsler CD; Shaw LN; Baker BJ Org. Lett 2016, 18, 2596–2599. [PubMed: 27175857]

(6). Baker BJ; Kopitzke RW; Yoshida WY; McClintock JB J. Nat. Prod 1995, 58, 1459–1462.

(7). van Soest R Personal communication.

(8). Keyzers RA; Northcote PT; Davies-Coleman MT Nat. Prod. Rep 2006, 23, 321–334. [PubMed: 16572231]

(9). van Griensven J; Diro E Infect. Dis. Clin. North Am 2019, 33, 79–99. [PubMed: 30712769]

(10). Joice AC; Yang S; Farahat AA; Meeds H; Feng M; Li J; Boykin DW; Wang MZ; Werbovetz KA Antimicrob. Agents Chemother 2018, 62, DOI: 10.1128/AAC.01129-17.

(11). Kanwar A; Eduful BJ; Barbeto L; Carletti Bonomo P; Lemus A; Vesely BA; Mutka TS; Azhari A; Kyle DE; Leahy JW ACS Med. Chem. Lett 2017, 8, 797–801. [PubMed: 28835791]

(12). Demers DH; Knestrick MA; Fleeman R; Tawfik R; Azhari A; Souza A; Vesely B; Netherton M; Gupta R; Colon BL; Rice CA; Rodriguez-Perez MA; Rohde KH; Kyle DE; Shaw LN; Baker BJ Mar. Drugs 2018, 16, 376.

(13). Tchokouaha Yamthe LR; Appiah-Opong R; Tsouh Fokou PV; Tsabang N; Fekam Boyom F; Nyarko AK; Wilson MD Mar. Drugs 2017, 15, No. e323. [PubMed: 29109372]

(14). Karuso P; Skelton BW; Taylor WC; White AH Aust. J. Chem 1984, 37, 1081–1093.

(15). Karuso P; Bergquist PR; Cambie RC; Buckleton JS; Clark GR; Rickard CEF Aust. J. Chem 1986, 39, 1643–1653.

(16). Graham SK; Garson MJ; Bernhardt PV J. Chem. Crystallogr 2010, 40, 468–471.

(17). Bruker. APEX3 2015.9 ed; Bruker AXS Inc.: Madison, WI, USA, 2016.

(18). Bruker. SAINT 8.35A ed; Bruker AXS Inc.: Madison, WI, USA, 2016.

(19). Sheldrick GM SADABS, Program for Empirical Absorption Correction; University of Gottingen, 1996.

(20). Sheldrick GM Acta Crystallogr., Sect. A: Found. Crystallogr 2008, A64, 112–122.

(21). Sheldrick GM Acta Crystallogr., Sect. A: Found. Crystallogr 2015, C71, 3–8.

(22). Dolomanov OV; Bourhis LJ; Gildea RJ; Howard JAK; Puschmann H J. Appl. Crystallogr 2009, 42, 339–341.

(23). Spek AL Acta Crystallogr., Sect. D: Biol. Crystallogr 2009, D65, 148–155. [PubMed: 19171970]

(24). Hooft RWW; Straver LH; Spek AL J. Appl. Crystallogr 2008, 41, 96–103. [PubMed: 19461838]

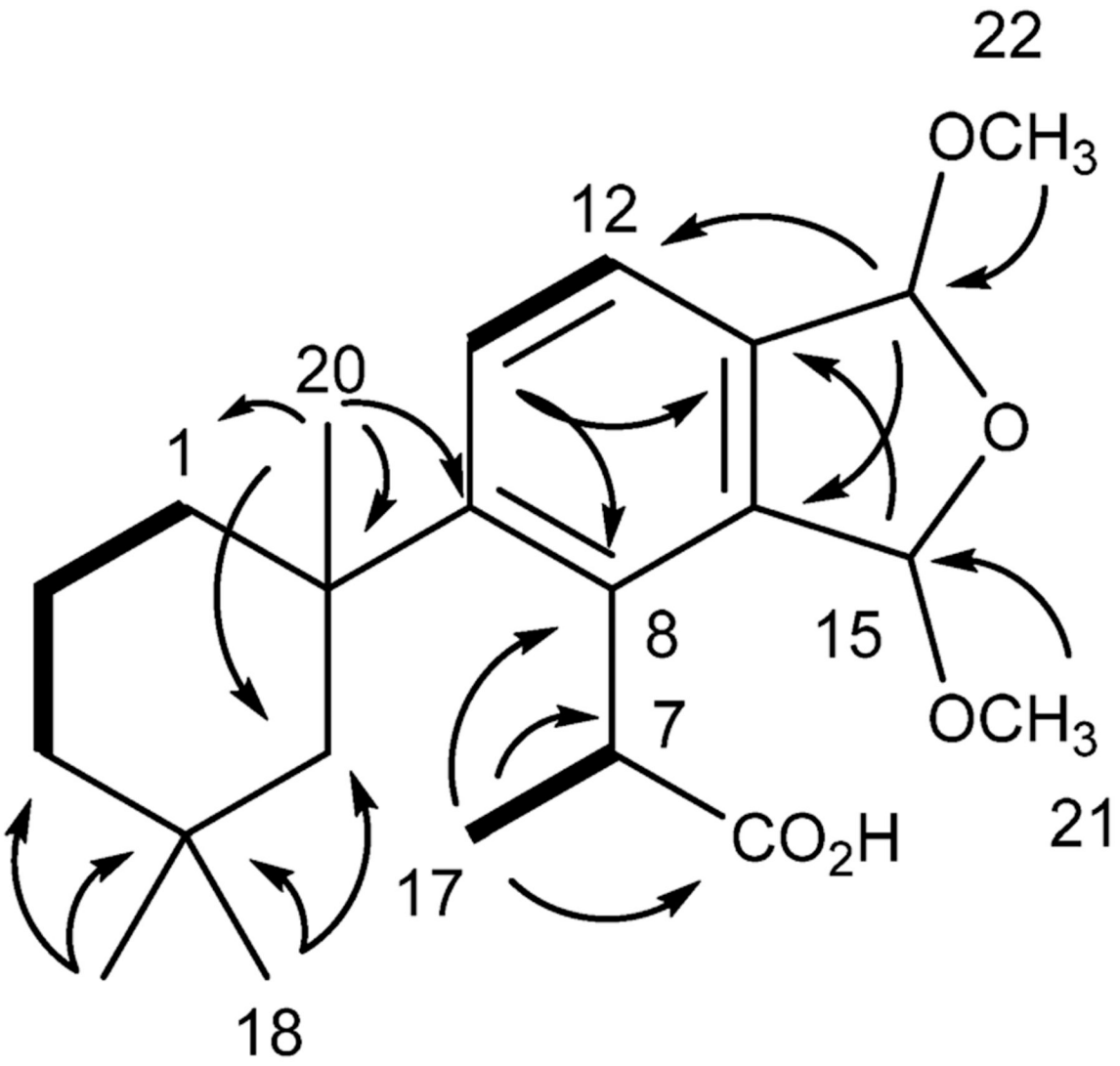

Figure 1.
Key HMBC (→) and COSY (—) correlations establishing the planar structure for membranoids B–E (**6**–**9**).

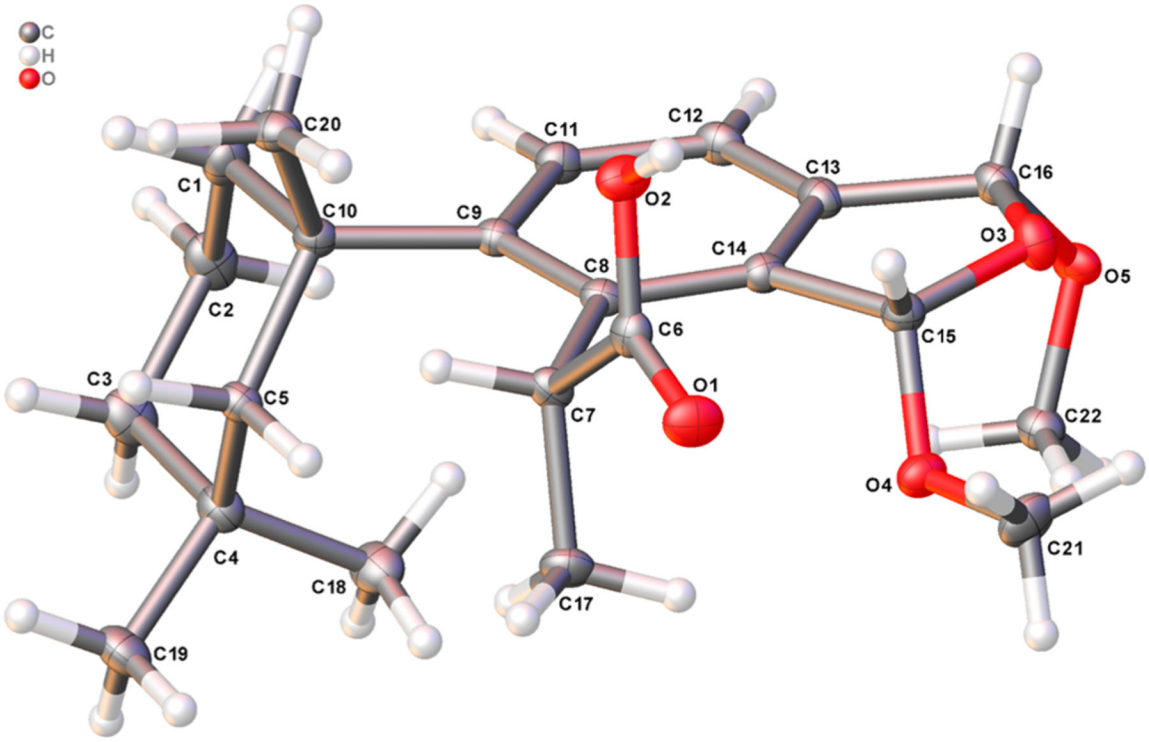

Figure 2.

X-ray crystal structure depicting the absolute configuration of membranoid C (**7**). Anisotropic displacement parameters are drawn at 50% probability.

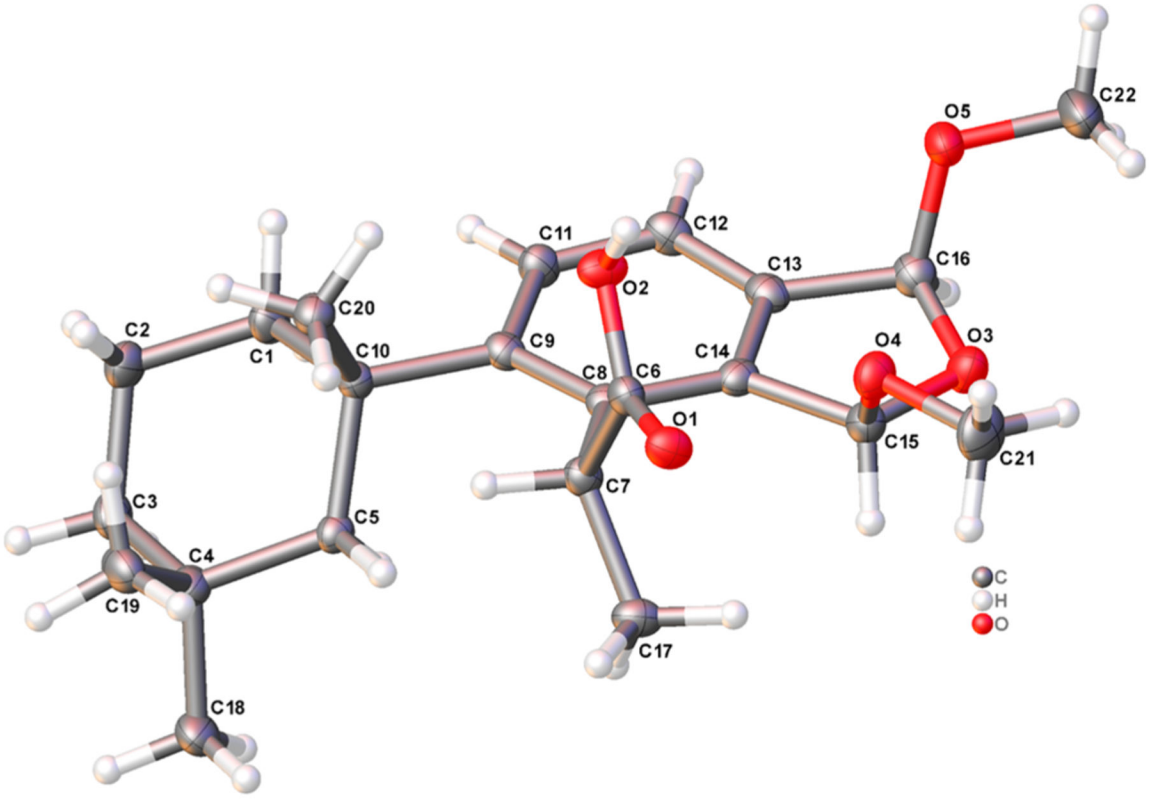

Figure 3.

X-ray crystal structure depicting the absolute configuration of membranoid E (**9**). Anisotropic displacement parameters are drawn at 50% probability.

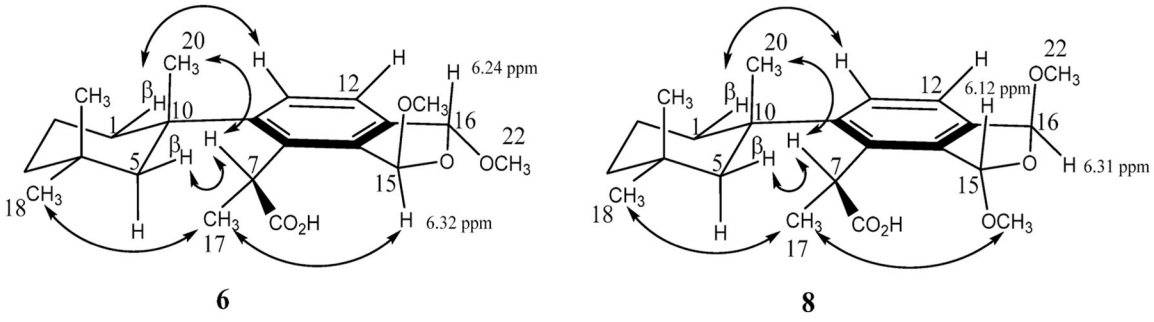

Figure 4.

NOESY correlations (CD_3CN) and ^1H NMR shifts ($CDCl_3$) establishing the relative configurations of membranoids B (**6**) and D (**8**).

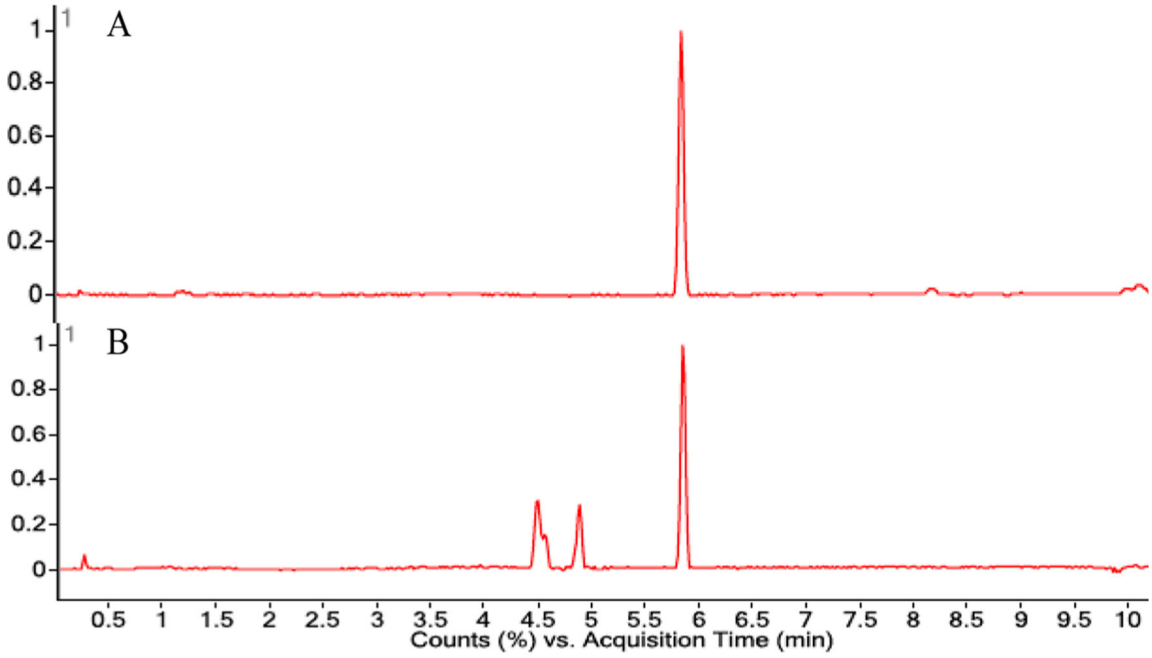

Figure 5.

LCMS chromatograms of (A) aplysulphurin (**1**) and (B) the emergence of new peaks (4.5–5.0 min) with masses matching the membranoids (**5**–**10**), after 12 h in MeOH.

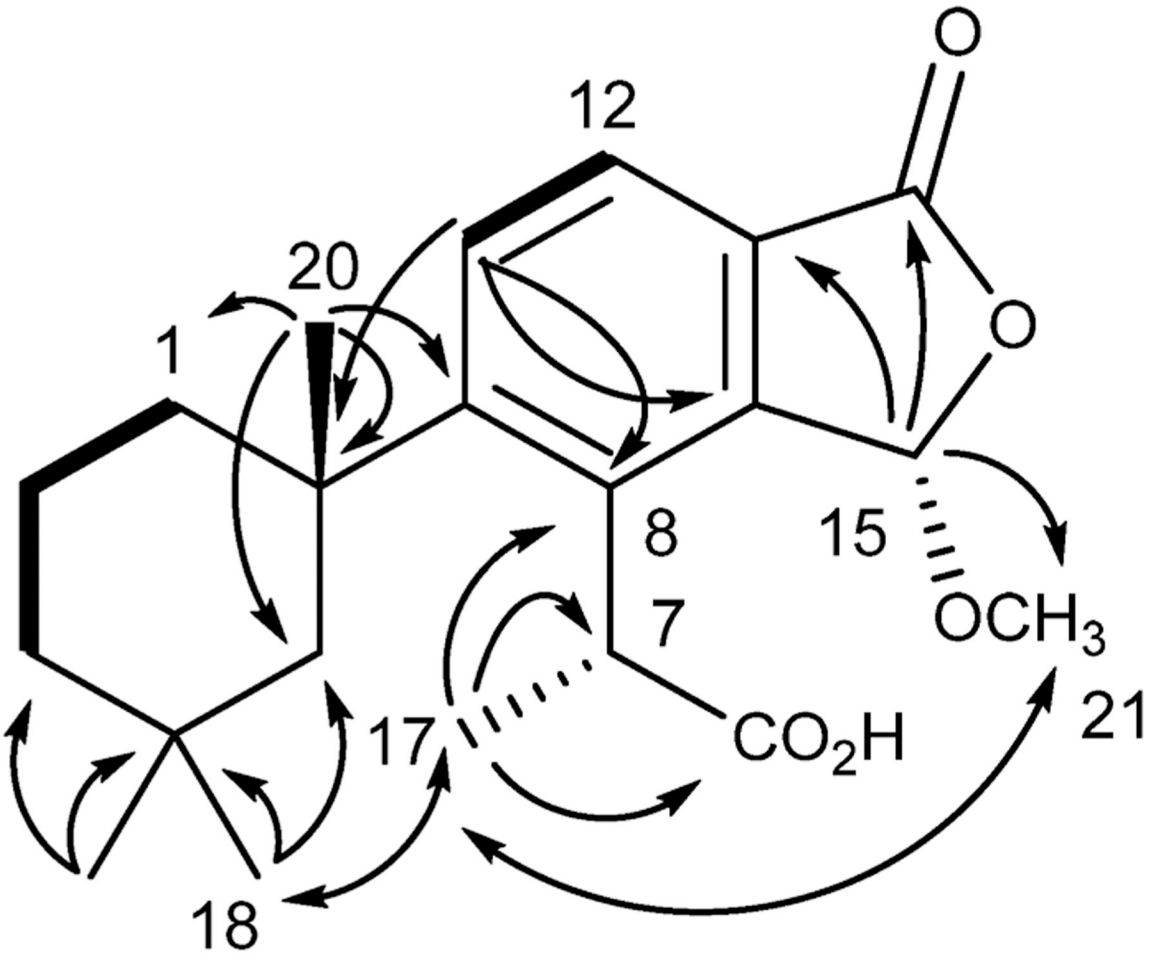

Figure 6.
Key HMBC (→), COSY (—), and ROESY (↔) correlations for membranoid F (**10**).

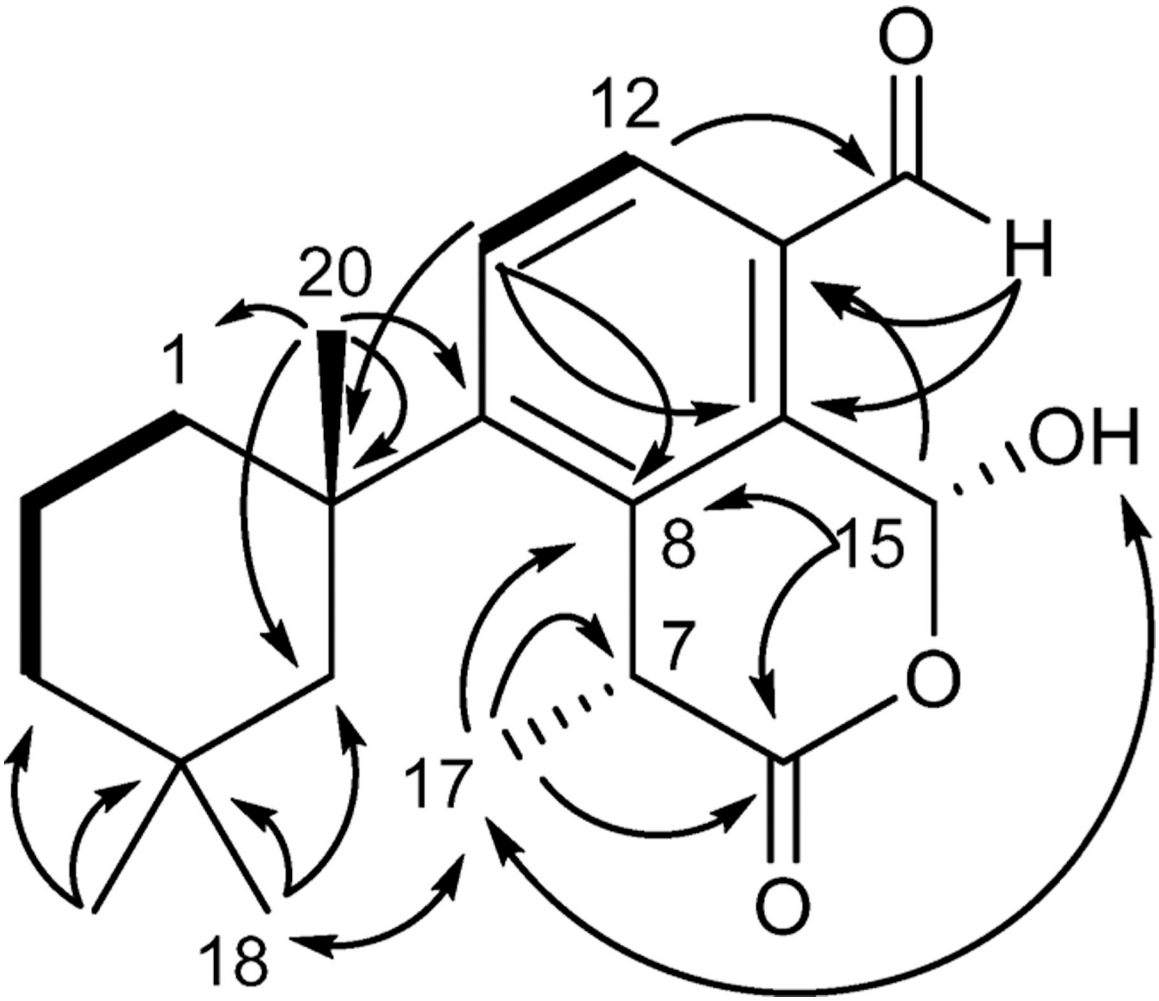

Figure 7.
Key HMBC (→), COSY (—), and NOESY (↔) correlations for membranoid G (**11**).

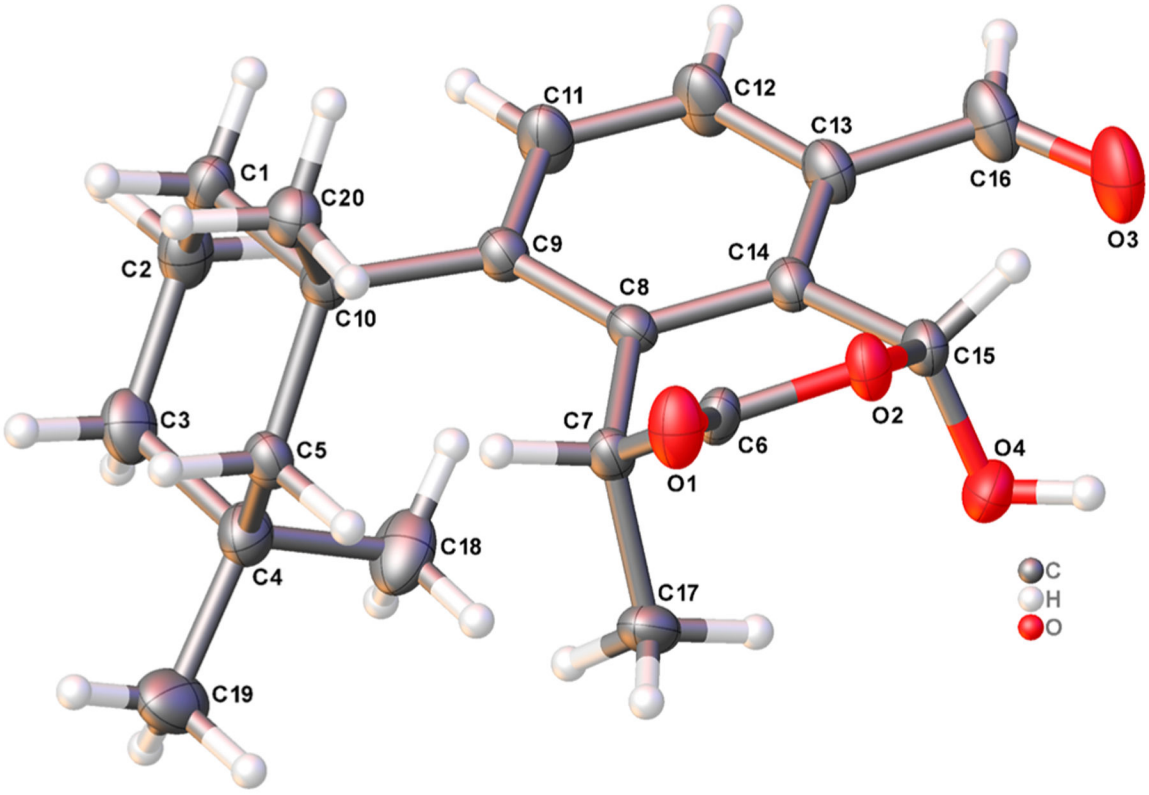

Figure 8.

X-ray crystal structure depicting the absolute configuration of membranoid G (**11**). Anisotropic displacement parameters are drawn at 50% probability.

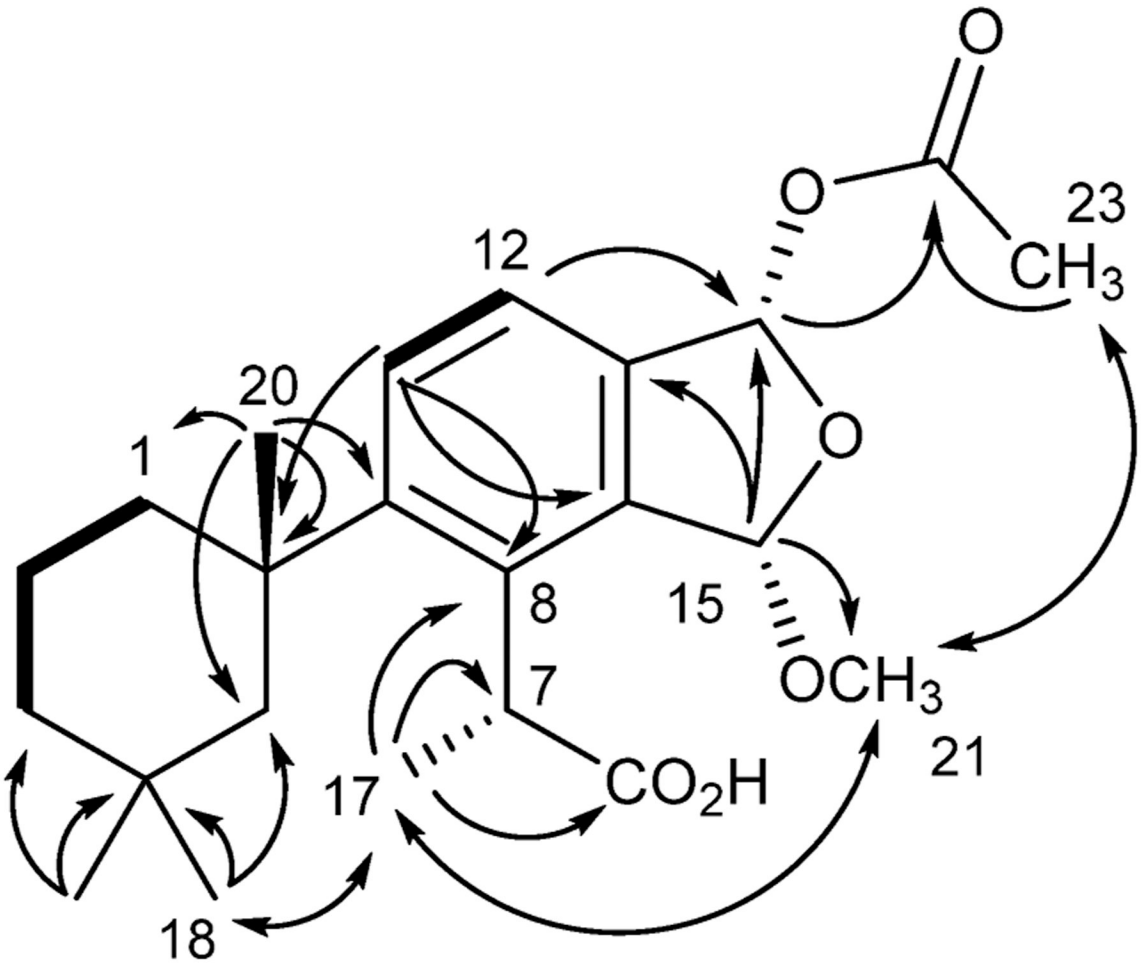

Figure 9.
Key HMBC (→), COSY (—), and NOESY (↔) correlations for membranoid H (**12**).

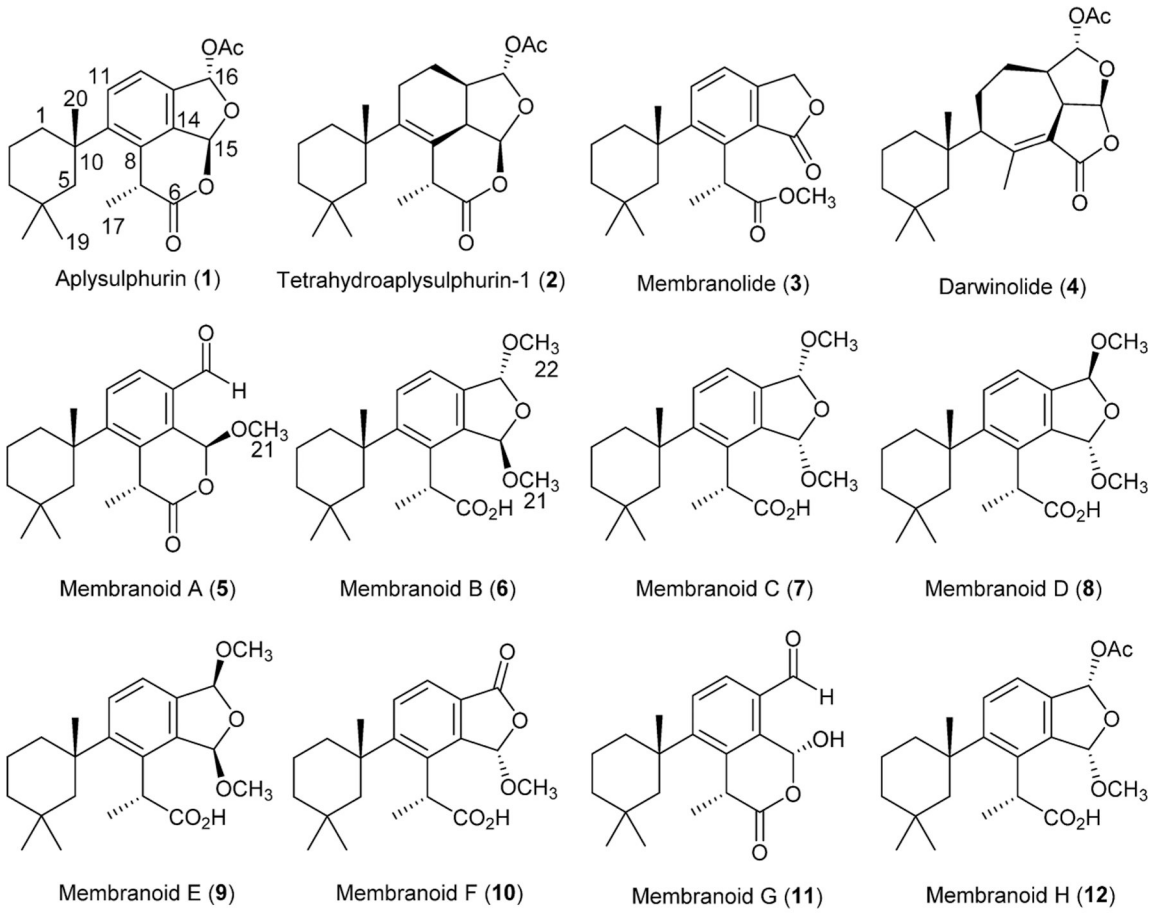

Chart 1.

Table 1.

NMR Data From Membranoids B–E (6–9)[a]

	membranoid B (6)		membranoid C (7)		membranoid D (8)		membranoid E (9)	
pos	δ_C, type[b]	δ_H[d] (*J* in Hz)	δ_C, type[c]	δ_H[e] (*J* in Hz)	δ_C, type[b]	δ_H[d] (*J* in Hz)	δ_C, type[c]	δ_H[e] (*J* in Hz)
1α	41.2, CH_2	1.45, ov dt	41.3, CH_2	1.46, ov dt	41.3, CH_2	1.47, ov dt	41.2, CH_2	1.47, ov, m
β		2.32, d (14.0)		2.31, d (14.0)		2.30, d (14.2)		2.33, d (14.5)
2α	20.0, CH_2	1.64, ov m	20.0, CH_2	1.66, ov m	20.0, CH_2	1.67, ov m	19.9, CH_2	1.64, ov, m
β		1.78, ov dd		1.82, ov dd		1.80, ov dd		1.77, ov, m
3	39.6, CH_2	1.27, ov m	39.9, CH_2	1.31, ov m	39.9, CH_2	1.29, ov m	39.6, CH_2	1.27, ov, m
4	31.7, C		31.8, C		31.8, C		31.7, C	
5α	51.0, CH_2	1.47, d (14.2)	50.6, CH_2	1.51, d (14.1)	50.5, CH_2	1.51 d, (14.1)	50.9, CH_2	1.47, ov, m
β		2.00, d (14.2)		2.10, d (14.1)		2.08, d (14.1)		1.99, d (13.6)
6	178.8, C		180.1, C		179.8, C		179.8, C	
7	40.0, CH	4.64, q (7.0)	41.2, CH	4.71, q (7.0)	41.3, CH	4.68, q (7.2)	40.0, CH	4.63, q (7.1)
8	135.7, C		135.7, C		135.8, C		135.6, C	
9	148.5, C		148.6, C		148.8, C		148.2, C	
10	39.3, C		39.5, C		39.5, C		39.3, C	
11	129.3, CH	7.58, d (8.3)	128.9, CH	7.58, d (8.3)	128.9, CH	7.57, d (8.3)	129.0, CH	7.56, d (8.3)
12	121.4, CH	7.24, d (8.3)	121.6, CH	7.26, d (8.3)	121.4, CH	7.23, d (8.3)	121.3, CH	7.21, d (8.3)
13	137.1, C		137.3, C		137.5, C		136.5, C	
14	138.4, C		139.5, C		139.6, C		138.4, C	
15	106.2, CH	6.32, d (1.8)	105.4, CH	5.89, s	106.2, CH	6.12, d (1.5)	105.6, CH	6.02, s
16	105.9, CH	6.24, d (1.8)	105.1, CH	5.89, s	105.6, CH	6.31, d (1.5)	104.5, CH	6.02, s
17	15.1, CH_3	1.58, d (7.2)	16.8, CH_3	1.73, d (7.2)	17.0, CH_3	1.71, d (7.2)	14.6, CH_3	1.57, d (7.2)
18	27.3, CH_3	0.36, s	27.4, CH_3	0.49, s	27.5, CH_3	0.49, s	27.3, CH_3	0.34, s
19	32.9, CH_3	0.90, s	32.8, CH_3	0.94, s	32.7, CH_3	0.94, s	32.9, CH_3	0.90, s
20	32.9, CH_3	1.44, s	33.0, CH_3	1.41, s	32.9, CH_3	1.41, s	32.8, CH_3	1.46, s
21	55.6, CH_3	3.40, s	54.7, CH_3	3.49, s	54.6, CH_3	3.45, s	55.6, CH_3	3.37, s
22	54.2, CH_3	3.40, s	54.8, CH_3	3.52, s	53.4, CH_3	3.33, s	52.8, CH_3	3.30, s

[a] $CDCl_3$.

[b] 125 MHz.

[c] 150 MHz.

[d] 500 MHz.

[e] 600 MHz; ov = overlapped.

Table 2.

NMR Data From Membranoids F (10),[a] G (11),[a] and H (12)[b]

	membranoid F (10)		membranoid G (11)		membranoid H (12)	
pos	**δ_C, type[c]**	**δ_H[d] (*J* in Hz)**	**δ_C, type[c]**	**δ_H[d] (*J* in Hz)**	**δ_C, type[c]**	**δ_H[d] (*J* in Hz)**
1α	41.2, CH_2	1.50, ov m	39.8, CH_2	1.52, m	41.9, CH_2	1.45, ov m
β		2.32, d (13.7)		2.23, m		2.33, d (14.3)
2α	19.9, CH_2	1.69, ov m	19.9, CH_2	1.73, m	20.8, CH_2	1.67, m
β		1.80, m		1.80, m		1.79, m
3α	39.7, CH_2	1.33, ov m	39.8, CH_2	1.33, m	40.5, CH_2	1.31, m
4	31.8, C		31.8, C		32.4, C	
5α	50.6, CH_2	1.55, d (14.2)	50.5, CH_2	1.59, m	50.9, CH_2	1.52, m
β		2.13, d (14.2)		2.06, m		2.16, d (14.2)
6	177.6, C		174.3, C		175.6, C	
7	40.8, CH	4.73, q (6.7)	39.5, CH	4.56, q (7.3)	41.7, CH	4.64, q (7.2)
8	137.5, C		138.2, C		137.9, C	
9	154.9, C		154.4, C		150.1, C	
10	40.3, C		40.5, C		40.4, C	
11	130.3, CH	7.76, d (8.3)	128.4, CH	7.76, d (8.3)	122.4, CH	7.65, d (8.3)
12	123.9, CH	7.73, d (8.3)	134.1, CH	7.73, d (8.3)	130.2, CH	7.30, d (8.3)
13	126.0, C		130.5, C		137.5, C	
14	145.1, C		134.0, C		140.8, C	
15	103.6, CH	6.14, s	92.9, CH	7.26, s	107.4, CH	5.86, s
16	168.6, C		192.5, CH	10.1, s	97.7, CH	6.98, s
17	17.7, CH_3	1.73, d (7.3)	24.2, CH_3	1.87, d (7.1)	17.6, CH_3	1.63, d (7.1)
18	27.3, CH_3	0.48, s	28.2, CH_3	0.58, s	27.5, CH_3	0.47, s
19	32.7, CH_3	0.95, s	32.2, CH_3	0.97, s	33.2, CH_3	0.93, s
20	32.7, CH_3	1.42, s	32.4, CH_3	1.32, s	33.3, CH_3	1.38, s
21	56.5, CH_3	3.59, s			55.3, CH_3	3.39, s
22					171.2, C	
23					21.5, CH_3	2.06, s

	membranoid F (10)		membranoid G (11)		membranoid H (12)	
pos	δ_C, type[c]	δ_H[d] (*J* in Hz)	δ_C, type[c]	δ_H[d] (*J* in Hz)	δ_C, type[c]	δ_H[d] (*J* in Hz)
OH				5.00, bs		

[a] $CDCl_3$.

[b] CD_3CN.

[c] 125 MHz.

[d] 500 MHz; ov = overlapped.

Table 3.

Bioactivity of *D. antarctica*-Derived Spongian Diterpenes and Their Methanolysis Products (IC_{50}, μM)

compound	*Leishmania donovani* IM	cytotoxicity (J774A.1)
aplysulphurin (**1**)	3.1	12.3
tetrahydroaplysulphurin-1 (**2**)	3.5	>133
membranolide (**3**)	9.7	76.8
darwinolide (**4**)	11.2	73.4
membranoid A (**5**)	>29.0	54.6
membranoid B (**6**)	0.8	>133
membranoid C (7)	6.5	>133
membranoid D (**8**)	1.4	>133
membranoid E (**9**)	6.6	95.0
membranoid F (**10**)	26.7	42.4
membranoid G (**11**)	1.9	>150
membranoid H (**12**)	12.0	62.9

[a]Positive control, miltefosine = 2.9 μM (IM), >120 μM (Cytotox).